Analysis of the Short-Time Unbiased Spectrum Estimation Algorithm

V. JOHN MATHEWS, MEMBER, IEEE, AND DAE-HEE YOUN, MEMBER, IEEE

Abstract—The short-time unbiased spectrum estimation (STUSE) algorithm is analyzed and expressions for the mean and variance of the spectrum estimates are derived. The STUSE algorithm deliberately adds biased spectrum estimates in order to yield unbiased estimates and at the same time have excellent spectral leakage suppression capabilities. Computer simulations are presented, verifying the theoretical results and also comparing the STUSE algorithm with the conventional weighted, overlapped, segment averaging (WOSA) method.

I. Introduction

Conventional methods of spectrum estimation have commonly employed the weighted, overlapped, segment averaging (WOSA) algorithm [1]-[3]. While the WOSA algorithm is computationally and statistically attractive, because of the inherent windowing involved in discrete Fourier transform (DFT) computations, the estimates are biased and also suffer from reduced spectral resolution. The short-time unbiased spectrum estimation (STUSE) algorithm [4]-[6] was proposed recently to overcome the above limitations of the WOSA algorithm by overlap adding biased spectrum estimates. The STUSE algorithm has been shown to be a very effective method for FIR system identification [4]-[6]. FIR system identification using the STUSE algorithm has the property that the solution to the system identification problem quickly approaches the theoretically optimum least squares solution as the number of samples used in the estimate increases [4], [6]. The usefulness of the STUSE algorithm for estimating time delay and magnitude-squared coherence function has been demonstrated in [7]. However, many statistical properties of this algorithm are still little understood.

In this paper, we derive analytical expressions for the estimation variance of the STUSE algorithm and verify the analysis using computer simulations. We also show that the effective window function [8] for the STUSE algorithm is uniformly superior [9] to the effective window function for the WOSA algorithm, implying that the STUSE algorithm suppresses spectral leakage better than the WOSA algorithm when both the methods use the same linear window function. We also present a theoretical and empirical comparison of the variance of the estimates obtained using the STUSE and WOSA algorithms. It will be shown by means of an example that the STUSE algorithm exhibits smaller estimation variance than the WOSA algorithm when the statistical bandwidth [10] of the effective windows for both the algorithms are the same.

Manuscript received February 27, 1984; revised August 27, 1984.
The authors are with the Department of Electrical and Computer Engineering, The University of Iowa, Iowa City, IA 52240.

The organization of the paper is as follows. In the next section, we review the WOSA method and present the STUSE algorithm. Expressions for the estimation variance, assuming Gaussian time series, are derived in Section III. Simulation examples verifying the theoretical results in earlier sections are presented in Section IV. Section V contains a summary of the results and concluding remarks.

II. Past Work and the STUSE Algorithm

Let $x_1(k)$ and $x_2(k)$ for $k = 0, 1, \cdots, P-1$ be two stationary time series. The $2M$-point cross-power density spectrum (cross-PDS) between $x_1(k)$ and $x_2(k)$ (if $x_1(k) = x_2(k)$ for all k, we get the auto-PDS) is defined as

$$G_{12}(f\cdot\Delta_{2M}) = F_{2M}\{c_{12}(m)\}; \quad m = -M, -M+1, \cdots, M-1, \quad f = 0, 1, 2, \cdots, 2M-1 \tag{1}$$

where

$$c_{12}(m) = E\{x_1(k)\, x_2(k-m)\} \tag{2}$$

is the crosscorrelation function between $x_1(k)$ and $x_2(k)$, $F_{2M}\{\cdot\}$ denotes the $2M$-point discrete Fourier transform of $\{\cdot\}$, $E\{\cdot\}$ denotes the statistical expectation of $\{\cdot\}$,

$$\Delta_{2M} = f_s/2M, \tag{3}$$

f_s is the sampling frequency in Hz, and f is a discrete integer frequency index.

In the WOSA method one segments $x_1(k)$ and $x_2(k)$ into N overlapped segments of length L_1 each, applies a linear window function $w(n)$ multiplicatively to each segment, and computes the $2M$-point DFT of the lth weighted segment of $x_i(k)$ as

$$X_{i,l}(f\cdot\Delta_{2M}) = F_{2M}\{x_i(lR+n)\, w(n)\} \quad \text{for } 0 \leqslant n \leqslant L_1 - 1, \quad 0 \leqslant l \leqslant N-1, \quad i = 1 \text{ or } 2 \text{ and } M \geqslant L_1, \tag{4}$$

where R denotes the number of samples between successive segments (i.e., $L_1 - R$ samples are overlapped). The cross-PDS between $x_1(k)$ and $x_2(k)$ is now estimated as

$$\hat{G}_{12}^{(w)}(f\cdot\Delta_{2M}) = \frac{1}{N}\cdot\frac{1}{(2M)}\cdot\frac{1}{r_{ww}(0)} \cdot \sum_{l=0}^{N-1} X_{1,l}(f\cdot\Delta_{2M})\, X_{2,l}^{*}(f\cdot\Delta_{2M}) \tag{5}$$

where

$$r_{ww}(k) = \frac{1}{2M} \sum_{n=0}^{L_1-1} w(n)\, w(n-k), \tag{6}$$

carets denote estimated quantities, and "*" denotes complex conjugate.

It has been shown [2], [3] that the expected value of $\hat{G}_{12}^{(w)}(f \cdot \Delta_{2M})$,

$$E\{\hat{G}_{12}^{(w)}(f \cdot \Delta_{2M})\} = G_{12}(f \cdot \Delta_{2M}) \circledast \frac{G_{ww}(f \cdot \Delta_{2M})}{r_{ww}(0)} \tag{7}$$

where $G_{ww}(f \cdot \Delta_{2M})$ is the $2M$-point auto-PDS of the linear window function $w(n)$, and $\circledast$ denotes complex convolution.

From (7) we can see that for $\hat{G}_{12}^{(w)}(f \cdot \Delta_{2M})$ to be unbiased, $G_{ww}(f \cdot \Delta_{2M})$ should be a delta function. However, for all the finite length linear window functions, $G_{ww}(f \cdot \Delta_{2M})$ exhibits low-pass characteristics and the estimate in (5) is biased. Recently, a new spectrum estimation technique has been proposed, in which the influence of the finite window length on a spectral estimate can be removed by linearly combining biased estimates [4]-[6]. This method, which has been referred to as the STUSE algorithm [4] computes the cross-PDS between $x_1(k)$ and $x_2(k)$ as

$$\hat{G}_{12}^{(s)}(f \cdot \Delta_{2M}) = \sum_{q=Q_1}^{Q_2} \hat{G}_{12,q}(f \cdot \Delta_{2m})\, e^{j(2\pi/2M)fRq} \tag{8}$$

where

$$\hat{G}_{12,q}(f \cdot \Delta_{2M}) = \frac{1}{N} \cdot \frac{1}{2M} \cdot \frac{1}{\tilde{r}_{ww}(0)} \cdot \sum_{l=0}^{N-1} X_{1,l}(f \cdot \Delta_{2M}) \cdot X_{2,l+q}^{*}(f \cdot \Delta_{2M}) \tag{9}$$

and

$$\tilde{r}_{ww}(m) = \sum_{q=Q_1}^{Q_2} r_{ww}(m+qR). \tag{10}$$

In (8) the exponential term takes care of the time delay between the nth and $(n+q)$th segments. It is assumed here that the product of $\tilde{r}_{ww}(m)$ and the cross-correlation function of $x_1(k)$ and $x_2(k)$ is zero for $|m| > M$, i.e.,

$$c_{11}(m) \cdot \tilde{r}_{ww}(m) = 0; \qquad |m| > M. \tag{11}$$

As for the case of the WOSA method, we can show that the expected value of the cross-PDS estimate using the STUSE algorithm is given by

$$E\{\hat{G}_{12}^{(s)}(f \cdot \Delta_{2M})\} = G_{12}(f \cdot \Delta_{2M}) \circledast \frac{\tilde{G}_{ww}(f \cdot \Delta_{2M})}{\tilde{r}_{ww}(0)} \tag{12a}$$

where

$$\tilde{G}_{ww}(f \cdot \Delta_{2M}) = \sum_{q=Q_1}^{Q_2} G_{ww}(f \cdot \Delta_{2M}) \cdot e^{j(2\pi/2M)\, fqR} = F_{2M}\{\tilde{r}_{ww}(m)\}. \tag{12b}$$

Thus, from (12a) and (12b), we can see that if Q_1, Q_2, and R are chosen carefully to have constant $\tilde{r}_{ww}(m)$ for $|m| \leq M$, the estimate $\hat{G}_{12}^{(s)}(f \cdot \Delta_{2M})$ in (8) obtained using the STUSE algorithm is unbiased.

For $\tilde{r}_{ww}(m)$ to be flat in a given range, Q_1 and Q_2 should be large enough and R should be chosen such that 1) $R = 1$, 2) the auto-PDS of $w(n)$ is zero for nonzero integer multiples of $(1/R)$ (this implies that rectangular windows require no overlap, Hanning windows require 50 percent overlap, Blackman windows require 75 percent overlap, and so on [11]), or 3) R is smaller than the "Nyquist" sampling interval of the band-limited window function $w(n)$ [12]. In many cases, the window functions will neither be band limited nor be such that it is zero at nonzero multiples of some fundamental frequency. Also, since most of the discrete window functions are numerically evaluated, errors in numerical computations may give the window functions nonzero values at frequencies where they should have zero value theoretically. In such cases, these window functions may be considered approximately band limited and the shift R may be chosen such that $(1/R)$ is at least twice the approximate bandwidth. Thus R may be chosen to be less than or equal to one-fourth the window length if we consider the -42 dB bandwidth of Hamming window functions [4]-[6]. For a comprehensive study of window functions, one may refer to [13]-[15].

If R is chosen as above, and

$$-Q_1 = Q_2 = \left\lfloor \frac{M+L_1}{R} \right\rfloor \tag{13}$$

where $\lfloor(\cdot)\rfloor$ is the largest integer smaller than $(\cdot)$, we have

$$\tilde{r}_{ww}(m) = \tilde{r}_{ww}(0); \qquad |m| \leq M. \tag{14}$$

This is true since shifts beyond Q_1 and Q_2 does not have any influence on $\tilde{r}_{ww}(m)$ for $|m| \leq M$. Now, if

$$c_{12}(m) = 0; \qquad |m| > M \tag{15}$$

we have

$$E\{\hat{G}_{12}^{(s)}(f \cdot \Delta_{2M})\} = F_{2M}\left\{\frac{c_{12}(m) \cdot \tilde{r}_{ww}(m)}{\tilde{r}_{ww}(0)}\right\} \tag{16a}$$

$$= F_{2M}\{c_{12}(m)\} \tag{16b}$$

$$= G_{12}(f \cdot \Delta_{2M}) \tag{16c}$$

thus yielding unbiased estimates of the cross-PDS.

Remarks:

1) The STUSE algorithm with $Q_1 = Q_2 = 0$ is identical to the WOSA algorithm. Thus the STUSE algorithm may be viewed as a generalization of the WOSA algorithm and therefore, all the analysis in this paper apply to the WOSA algorithm also.

2) If (11) does not hold, the algorithm may be modified as follows [7]. For $q = Q_1, \cdots, Q_2$, define

$$\hat{c}_{12,q}(m) = F_{2M}^{-1}\{\hat{G}_{12,q}(f \cdot \Delta_{2M})\} \tag{17}$$

where $F^{-1}\{\cdot\}$ denotes the $2M$-point inverse of $\{\cdot\}$. Now compute the spectrum as

$$\hat{G}_{12}^{(s)}(f \cdot \Delta_{2K_1}) = F_{2K_1}\left\{ \sum_{q=Q_1}^{Q_2} \hat{c}_{12,q}(m+qR) \right\}. \tag{18}$$

Note that $|m|$ may be larger than M and that the final FFT length $2K_1$ may be larger than the one used to obtain $\hat{G}_{12,q}(f \cdot \Delta_{2M})$ (i.e., $2M$). In (18), the time shift qR corresponds to the exponential term in (7).

3) In (7) and (12a), $G_{ww}(f \cdot \Delta_{2M})$ and $\tilde{G}_{ww}(f \cdot \Delta_{2M})$ will be called the effective window functions for the WOSA and STUSE algorithms, respectively. Also, $r_{ww}(k)$ and $\tilde{r}_{ww}(k)$ will be referred to as the effective lag window functions for the WOSA and STUSE algorithms, respectively.

We will now show that even when Q_1 and Q_2 are not selected as in (13), $\tilde{G}_{ww}(f \cdot \Delta_{2M})$ has better sidelobe structure than $G_{ww}(f \cdot \Delta_{2M})$. That is,

$$\left| \frac{\tilde{G}_{ww}(f \cdot \Delta_{2M})}{\tilde{G}_{ww}(0)} \right| = \frac{\left| \sum_{q=Q_1}^{Q_2} G_{ww}(f \cdot \Delta_{2M})\, e^{j(2\pi/2M) fqR} \right|}{(Q_2 - Q_1 + 1)\, |G_{ww}(0)|} \tag{19a}$$

$$\leqslant \sum_{q=Q_1}^{Q_2} \frac{|G_{ww}(f \cdot \Delta_{2M})|\, |e^{j(2\pi/2M) fqR}|}{(Q_2 - Q_1 + 1)\, |G_{ww}(0)|} \tag{19b}$$

$$= \left| \frac{G_{ww}(f \cdot \Delta_{2M})}{G_{ww}(0)} \right|. \tag{19c}$$

Inequalities in (19a)-(19c) imply that the mainlobe width of $\tilde{G}_{ww}(f \cdot \Delta_{2M})$ is less than or equal to that of $G_{ww}(f \cdot \Delta_{2M})$ and that the sidelobes of the former are at most as large as that of the latter. That is, $\tilde{G}_{ww}(f \cdot \Delta_{2M})$ is uniformly superior [9] to $G_{ww}(f \cdot \Delta_{2M})$. Because of this, the STUSE algorithm suppresses spectral leakage better than the WOSA algorithm when both the methods use the same linear window.

In the next section we will derive analytical expressions for the variance of the spectrum estimates obtained using the STUSE algorithm.

III. Variance Analysis

We will assume that $\hat{G}_{12}^{(s)}(f \cdot \Delta_{2M})$ for $f = 0, 1, 2, \cdots, 2M - 1$ in (8) was obtained by first computing a $2L$-point intermediate spectrum $\hat{G}_{12}(f \cdot \Delta_{2L})$ for $f = 0, 1, 2, \cdots 2L - 1$ and then sampling $\hat{G}_{12}(f \cdot \Delta_{2L})$ every $K = L/M$ frequency bins. L is chosen such that $L \geqslant P$ and K is an integer. $\hat{G}_{12}^{(s)}(f \cdot \Delta_{2M})$ obtained by this procedure and by (8) and (9) are identical, since from (4)-(10)

$$\hat{G}_{12}(Kf \cdot \Delta_{2L}) = \frac{1}{\beta} \sum_{q=Q_1}^{Q_2} \sum_{l=0}^{N-1} \sum_{t_1, t_2=0}^{L_1-1} \cdot \{x_1(lR+t_1)\, x_2((l+q)R+t_2) \cdot w(t_1)\, w(t_2)\} \cdot e^{-j(2\pi/2L)\, Kf(t_1-t_2-qR)} \tag{20a}$$

$$= \frac{1}{\beta} \sum_{q=Q_1}^{Q_2} \sum_{l=0}^{N-1} \sum_{t_1, t_2=0}^{L_1-1} \cdot \{x_1(lR+t_1)\, x_2((l+q)R+t_2) \cdot w(t_1)\, w(t_2)\} \cdot e^{-j(2\pi/2M) f(t_1-t_2-qR)} \tag{20b}$$

$$= \hat{G}_{12}^{(s)}(f \cdot \Delta_{2M}) \quad \text{for } f = 0, 1, \cdots, 2M-1 \tag{20c}$$

where

$$\beta = N \cdot \sum_{q=Q_1}^{Q_2} \sum_{n=0}^{L_1-1} w(n)\, w(n-qR). \tag{21}$$

The above procedure is very useful for analysis since all the data segments may be correlated. This will become more apparent during the derivation. We will also assume that the data belong to a real stationary Gaussian time series.

Now the expected value of the product of $\hat{G}_{12,q_1}(f \cdot \Delta_{2L})$ and $\hat{G}_{12,q_2}^{*}(f \cdot \Delta_{2L})$ is given by

$$E\{\hat{G}_{12,q_1}(f \cdot \Delta_{2L})\, \hat{G}_{12,q_2}^{*}(f \cdot \Delta_{2L})\} = \frac{1}{N^2} \cdot \frac{1}{(2L)^2} \cdot \frac{1}{[\tilde{r}_{ww}(0)]^2} \cdot \sum_{l_1, l_2=0}^{N-1} \sum_{t_1, t_2, t_3, t_4=0}^{2L-1} \cdot E\{x_1(l_1R+t_1)\, x_2((l_1+q_1)R+t_2)\, x_1(l_2R+t_3) \cdot x_2((l_2+q_2)R+t_4)\} \cdot w(t_1)\, w^*(t_2)\, w^*(t_3)\, w(t_4) \cdot e^{-j(2\pi/2L)\{f(t_1-t_2-t_3+t_4)\}} \tag{22}$$

where $w(t)$ is taken to be zero for t greater than the window length and $\tilde{r}_{ww}(0)$ is defined with $2L$ in the denominator instead of $2M$ as in (6).

Because of Gaussianity, the expectation in (22) may be written as [16]

$$E\{\cdots\} = c_{12}(-q_1R+t_1-t_2)\, c_{12}(-q_2R+t_3-t_4) + c_{11}((l_1-l_2)R+t_1-t_3)\, c_{22}((l_1+q_1) - (l_2+q_2))R+t_2-t_4) + c_{12}((l_1-(l_2+q_2)) \cdot R+t_1-t_4)\, c_{12}((l_2-(l_1+q_1))R+t_3-t_2) \tag{23}$$

where

$$c_{ij}(m) = E\{x_i(t)\, x_j(t-m)\} \quad \text{for } i, j = 1, \text{or } 2. \tag{24}$$

Expressing $c_{ij}(m)$ as

$$c_{ij}(m) = \frac{1}{2L} \sum_{f=0}^{2L-1} G_{ij}(f \cdot \Delta_{2L})\, e^{j(2\pi/2L) fm} \tag{25}$$

and substituting (23) and (25) in (22) and simplifying, we obtain

$$E\{\hat{G}_{12,q_1}(f\cdot\Delta_{2L})\,\hat{G}^*_{12,q_2}(f\cdot\Delta_{2L})\}=\left\{G_{12}(f\cdot\Delta_{2L})\,e^{-j(2\pi/2L)fq_1R}\circledast\frac{|W(f\cdot\Delta_{2L})|^2}{2L\cdot\tilde{r}_{ww}(0)}\right\}\cdot\left\{G_{12}(f\cdot\Delta_{2L})\,e^{-j(2\pi/2L)fq_2R}\right.$$
$$\left.\circledast\frac{|W(f\cdot\Delta_{2L})|^2}{2L\cdot\tilde{r}_{ww}(0)}\right\}^*+\frac{1}{(2L)^2}\sum_{\mu,\nu=0}^{2L-1}G_{11}(\mu\cdot\Delta_{2L})\,G_{22}(\nu\cdot\Delta_{2L})\,\frac{|W((f-\mu)\cdot\Delta_{2L})\,W((f-\nu)\cdot\Delta_{2L})|^2}{(2L)^2\cdot\tilde{r}^2_{ww}(0)}$$
$$\cdot\left\{\sum_{l_1,l_2=0}^{N-1}e^{j(2\pi/2L)(l_1-l_2)R(\mu-\nu)}\right\}\cdot e^{-j(2\pi/2L)\nu(q_1-q_2)R}+\frac{1}{(2L)^2}\left\{\sum_{\mu,\nu=0}^{2L-1}G_{12}(\mu\cdot\Delta_{2L})\,G^*_{12}(\nu\cdot\Delta_{2L})\right\}$$
$$\cdot\left\{\frac{W((f-\mu)\cdot\Delta_{2L})\,W((f+\mu)\cdot\Delta_{2L})\,W^*((f+\nu)\cdot\Delta_{2L})\,W^*((f-\nu)\cdot\Delta_{2L})}{(2L)^2\,\tilde{r}^2_{ww}(0)}\right\}\cdot\left\{\sum_{l_1,l_2=0}^{N-1}e^{j(2\pi/2L)(l_1-l_2)R(\mu-\nu)}\right\}$$
$$\left.\cdot\,e^{-j(2\pi/2L)\mu q_2R+j(2\pi/2L)\nu q_1R}\right\}. \tag{26}$$

In the above expression, the exponential terms $\exp\{j(2\pi/2L)(l_1-l_2)R(\mu-\nu)\}$ take care of the dependence of the l_1th and l_2th segments on each other. If $L<P$, this expression will not give correct results, and hence the need for the analysis procedure described at the beginning of this section. The first term of (26) is the product of the expected values of $\hat{G}_{12,q_1}(f\cdot\Delta_{2L})$ and $\hat{G}_{12,q_2}(f\cdot\Delta_{2L})$ and the third term is negligibly small for all f except $f=0$ and $f=L$, for most choices of window functions [17]. Therefore, the covariance between $\hat{G}_{12,q_1}(f\cdot\Delta_{2L})$ and $\hat{G}_{12,q_2}(f\cdot\Delta_{2L})$ may be approximated as

$$\operatorname{cov}\{\hat{G}_{12,q_1}(f\cdot\Delta_{2L}),\ \hat{G}_{12,q_2}(f\cdot\Delta_{2L})\}\cong\frac{1}{(2L)^2}\sum_{\mu,\nu=0}^{2L-1}G_{11}(\mu\cdot\Delta_{2L})\,G_{22}(\nu\cdot\Delta_{2L})\cdot|\gamma(f-\mu,f-\nu)|^2\,S_1^2(\mu-\nu)\,e^{-j(2\pi/2L)\nu(q_1-q_2)R}$$
$$\text{for } f=0,1,2,\cdots,2L-1 \tag{27}$$

where

$$S_1^2(x)=\sum_{l_1,l_2=0}^{2L-1}e^{j(2\pi/2L)(l_1-l_2)Rx}=\left[\frac{\sin\left(\frac{\pi}{2L}RNx\right)}{N\cdot\sin\left(\frac{\pi}{2L}Rx\right)}\right]^2 \tag{28}$$

and

$$|\gamma(x,y)|^2=\left|\frac{W(x\cdot\Delta_{2L})\,W(y\cdot\Delta_{2L})}{2L\cdot\tilde{r}_{ww}(0)}\right|^2. \tag{29}$$

Now, using (8) and (27), the variance of the estimate $\hat{G}^{(s)}_{12}(f\cdot\Delta_{2L})$ is given by

$$\operatorname{var}\{\hat{G}^{(s)}_{12}(f\cdot\Delta_{2L})\}=\sum_{q_1,q_2=Q_1}^{Q_2}\operatorname{cov}\{\hat{G}_{12,q_1}(f\cdot\Delta_{2L}),\hat{G}_{12,q_2}(f\cdot\Delta_{2L})\}\,e^{j(2\pi/2L)fR(q_1-q_2)} \tag{30a}$$

$$=\frac{1}{(2L)^2}\sum_{\mu,\nu=0}^{2L-1}G_{11}(\mu\cdot\Delta_{2L})\cdot G_{22}(\nu\cdot\Delta_{2L})|\gamma(f-\mu,f-\nu)|^2\cdot S_1^2(\mu-\nu)\,S_2^2(f-\nu)$$
$$\text{for } f=0,1,\cdots,2L-1 \tag{30b}$$

where

$$S_2^2(x)=\left\{\frac{\sin\left(\frac{\pi}{2L}(Q_2-Q_1+1)Rx\right)}{\sin\left(\frac{\pi}{2L}Rx\right)}\right\}^2. \tag{31}$$

Since the $2M$-point spectrum $\hat{G}^{(s)}_{12}(f\cdot\Delta_{2M})$ is obtained by sampling the $2L$-point spectrum $\hat{G}^{(s)}_{12}(f\cdot\Delta_{2L})$ every K ($=L/M$) frequency bins, the variance of $\hat{G}^{(s)}_{12}(f\cdot\Delta_{2M})$ is given by

$$\operatorname{var}\{\hat{G}^{(s)}_{12}(f\cdot\Delta_{2M})\}=\frac{1}{(2L)^2}\sum_{\mu,\nu=0}^{2L-1}G_{11}(\mu\cdot\Delta_{2L})\cdot G_{22}(\nu\cdot\Delta_{2L})|\gamma(Kf-\mu,Kf-\nu)|^2\cdot S_1^2(\mu-\nu)\,S_2^2(Kf-\nu). \tag{32}$$

Equation (32) is exact, but for the approximation on the third term of (26). For $f=0$ and M, the variance is approximately twice that given by (32) since the second and third terms of (26) are equal at $f=0$ and L. We can make further approximations on (32) if $G_{11}(f\cdot\Delta_{2L})$ and $G_{22}(f\cdot\Delta_{2L})$ are relatively constant in a region of width equal to the statistical bandwidth of $\tilde{G}_{ww}(f\cdot\Delta_{2L})$ around the frequency of interest $f\cdot\Delta_{2M}$ as (see [17])

$$\operatorname{var}\{\hat{G}^{(s)}_{12}(f\cdot\Delta_{2M})\}\cong\frac{G_{11}(f\cdot\Delta_{2M})\,G_{22}(f\cdot\Delta_{2M})}{(2L)^2}\cdot\left[\sum_{\mu,\nu=0}^{2L-1}|\gamma(\mu,\nu)|^2\cdot S_1^2(\mu-\nu)\,S_2^2(\nu)\right]. \tag{33}$$

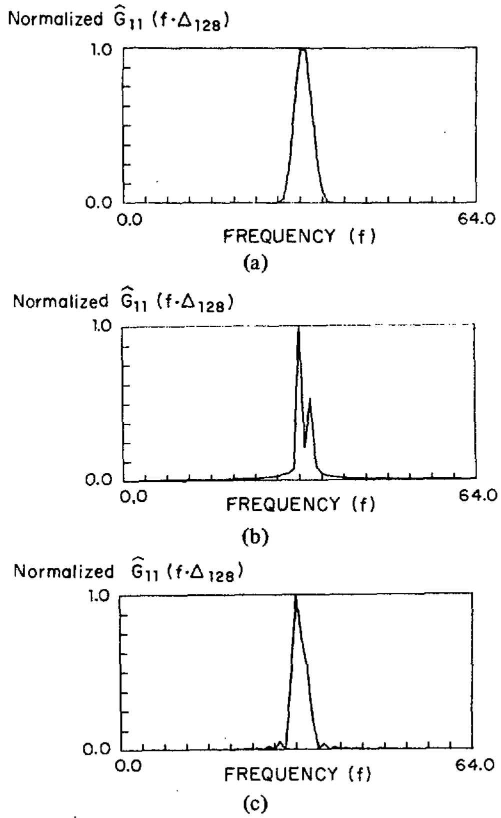

Fig. 1. Example comparing spectral resolution of the STUSE and WOSA algorithms. (a) WOSA with Hanning windows. (b) STUSE with Hanning windows. (c) WOSA with rectangular windows.

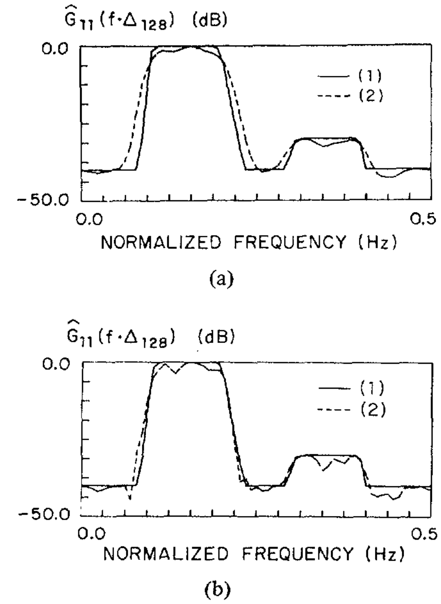

Fig. 2. Example demonstrating the good leakage suppression capability of the STUSE algorithm. (a): (1) true spectrum and (2) spectrum estimate using the WOSA algorithm. (b): (1) true spectrum and (2) spectrum estimate using the STUSE algorithm.

Thus, the normalized variance defined as

$$N\text{VAR}\,\{\hat{G}_{12}^{(s)}(f\cdot\Delta_{2M})\} \triangleq \frac{\text{var}\,\{\hat{G}_{12}^{(s)}(f\cdot\Delta_{2M})\}}{E\{\hat{G}_{11}^{(s)}(f\cdot\Delta_{2M})\}\,E\{\hat{G}_{22}^{(s)}(f\cdot\Delta_{2M})\}} \tag{34}$$

$$\cong \frac{1}{(2L)^2}\sum_{\mu,\nu=0}^{2L-1} |\gamma(\mu,\nu)|^2\, S_1^2(\mu-\nu)\, S_2^2(\nu) \tag{35}$$

is approximately independent of f.

IV. Simulation Examples

In this section, we will present four simulation examples, demonstrating the properties of the STUSE algorithm and verifying the theoretical results in the previous sections. The first example demonstrates the superior spectral resolution of the STUSE algorithm, when compared with the WOSA algorithm. The second example compares the spectral leakage suppression properties of the STUSE and WOSA algorithms. We verify the variance expressions derived in Section III, using example 3). A comparative study of the normalized variance of the estimates using the STUSE and WOSA algorithms as a function of the statistical bandwidth of the effective window functions is made in example 4).

Example 1): The signal used was the sum of two sinusoids of frequencies 32 and 33.75 Hz and amplitudes 2 and 1.5, respectively, sampled at 128 Hz. Fig. 1(a) displays the spectrum estimates normalized to have a maximum value of one, using the WOSA algorithm using 64-point Hanning windows, 128-point FFT's, 50 percent overlap, and 1024 data points. The corresponding estimates obtained with the STUSE algorithm using the same parameters as above, $-Q_1 = Q_2 = 2$ and using (18) are plotted in Fig. 1(b). For comparison, Fig. 1(c) shows the normalized spectrum estimate using the WOSA algorithm with 64-point rectangular windows, 128-point FFT's and 50 percent overlap. It may be noted that this case gives the best spectral resolution using the WOSA algorithm, for the parameters used. It can be seen that the WOSA algorithm cannot distinguish between the two frequency components, whereas the STUSE algorithm has good enough resolution to discriminate the two frequencies.

Example 2): The true auto-PDS of the signals used (in dB's) and normalized to have a maximum value of zero is plotted as curve 1 in both Fig. 2(a) and (b). Curve 2 in Fig. 2(a) and (b) are the estimates of the spectrum obtained using the WOSA and STUSE algorithms, respectively. Both the algorithms made use of 1024 data points, 64-point Hanning windows, 128-point FFT's, and 75 percent overlap ($R = 16$). For the STUSE algorithm, we used $-Q_1 = Q_2 = 2$ and (8). From Fig. 2(a) and (b), we can see that the STUSE algorithm exhibits better spectral leakage suppression capability than the WOSA algorithm. This property is significant since the STUSE algorithm alleviates one of the major drawbacks of linear windowing, namely bias, and at the same time retains its leakage suppression property. It may also be noted here that the estimate obtained using the STUSE algorithm is more noisy than that obtained using the WOSA algorithm. This is because the spectral resolution of the STUSE algorithm is better than that of the WOSA method in this example. However, we will see in example 4), that for the same spectral resolution of the estimates, the STUSE algorithm shows smaller variance than the WOSA method.

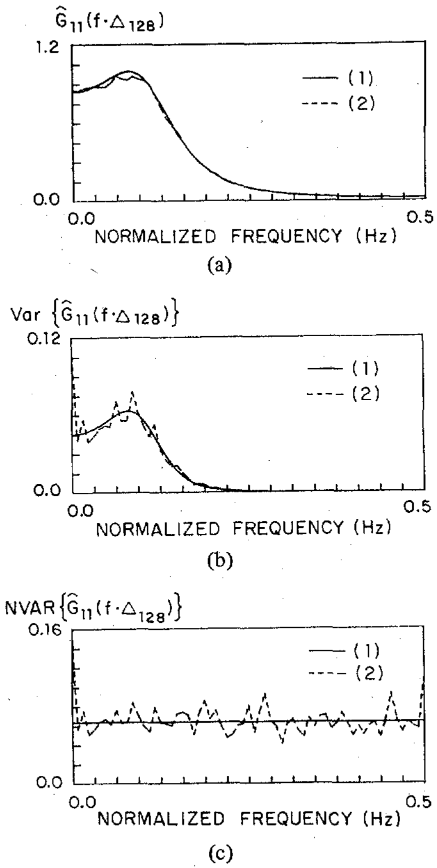

Fig. 3. Theoretical and empirical averages for example 3). (a): (1) true spectrum and (2) ensemble mean. (b): (1) theoretical variance and (2) ensemble variance. (c): (1) theoretical normalized variance and (2) ensemble normalized variance.

Example 3): In this example, we compute the auto power density spectrum of the signal obtained by passing a zero mean, Gaussian white signal through a second-order filter whose transfer function is given by

$$H(z) = \frac{0.367z^{-1}}{1 - z^{-1} + 0.4z^{-2}}. \quad (36)$$

The ensemble mean of eighty independent spectrum estimates using 1024 data points each obtained by the STUSE algorithm is displayed in Fig. 3(a), along with the true spectrum. We used 64-point Hanning windows, 128-point FFT's, 75 percent overlap and $-Q_1 = Q_2 = 2$ for the estimation using (8). Fig. 3(b) displays the ensemble variance of the estimates along with the theoretical variance given by (33). Also, plotted as Fig. 3(c) are the theoretical normalized variance given by (35) and the ensemble normalized variance. We can see that the correspondence between the simulation results and theoretical results is excellent. At $f = 0$ and 64, the ensemble variance is about twice the value given by (33), which is in accordance with the discussion after (32).

Example 4): We will now compare the normalized variance of the spectrum estimates obtained using the STUSE and WOSA algorithm as a function of the statistical bandwidth of the effective window function. The statistical bandwidth of the effective window function $W_e(f\cdot\Delta_{2M})$ is defined as [10]

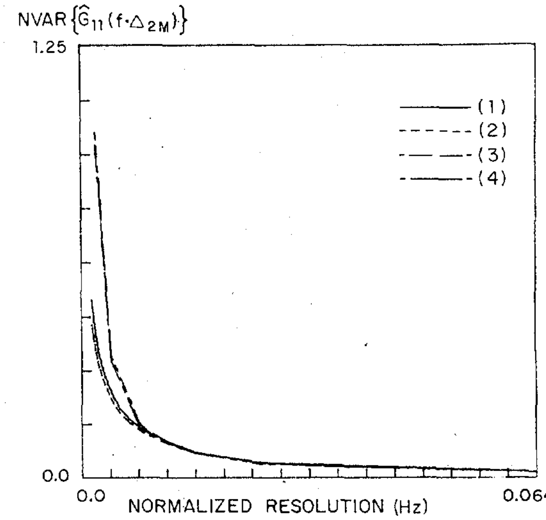

Fig. 4. Comparison of normalized variances of the estimates using the STUSE and the WOSA algorithms as a function of the normalized resolution of the estimates. (1) STUSE–theoretical, (2) STUSE–empirical, (3) WOSA–theoretical, and (4) WOSA–empirical.

$$B_e \triangleq \Delta_{2M} \cdot \frac{\left[\sum_{f=0}^{2M-1} W_e(f\cdot\Delta_{2M})\right]^2}{\sum_{f=0}^{2M-1} W_e^2(f\cdot\Delta_{2M})}. \quad (37)$$

The signals used were zero-mean white Gaussian with unit variance and forty independent estimates were made. The normalied variance was obtained as the average over all frequencies of the ensemble normalized variance. We used Hanning windows and 50 percent overlap for both the algorithms. For the STUSE algorithm, the linear window used was always a 32-point Hanning window function and the statistical bandwidth was varied by increasing $Q = -Q_1 = Q_2$ from 0 to 16. The FFT lengths $(2M)$ used to compute $\hat{G}_{12,q}(f\cdot\Delta_{2M})$ was 64, but the final FFT length $(2K_1)$ depended on Q. Equation (18) was used to compute all the estimates. The statistical bandwidth of the window function for the WOSA algorithm was varied by changing the window length L_1 from 32 to 1024. FFT lengths used were such that they were always greater than $2L_1$.

Fig. 4 displays the normalized variance obtained from the simulations for both the STUSE and WOSA algorithms as a function of the statistical bandwidth of their effective window functions as well as the corresponding theoretical curves given by (25). (Note that (33) is the same as (32) since the signal is white.) Once again, the agreement between theoretical and simulation results is excellent. We can see from the curves that for the same statistical bandwidth, the STUSE algorithm performs better than the WOSA algorithm from an estimation variance point of view.

V. Summary and Conclusions

The short-time unbiased spectrum estimation algorithm was analyzed and expressions for the variance of the spectrum estimates were derived. Simulation examples presented showed excellent agreement between analytical and simulation results.

We also showed that while the STUSE algorithm alleviates the problem of bias due to windowing, it retains the spectral leakage suppression capability of the linear window used. The last simulation result demonstrated that for the same statistical bandwidth of the effective window functions, the STUSE algorithm performs better than the WOSA algorithm, when the same type of linear windows and the same overlap between adjacent segments are used. However, this improvement in performance is achieved at the cost of higher computational cost. The statistical properties of the STUSE algorithm suggest that it is a viable and possibly better alternative for the WOSA algorithm, especially when computational considerations are not paramount. The usefulness of the STUSE algorithm in applications such as FIR system identification, time delay estimation, and magnitude-squared coherence function estimation, has already been documented in literature [4]-[7].

It may be pointed out that the variance analysis in Section III follows closely the work in [17]. However, the derivations in this paper are done completely in the discrete domain and therefore applicable to all values of FFT lengths, irrespective of the length of observation periods.

References

[1] P. D. Welch, "The use of FFT for the estimation of power spectra: A method based on time averaging over short modified periodograms," *IEEE Trans. Audio Electroacoust.*, vol. AU-15, pp. 70-73, June 1967.

[2] A. H. Nuttall, "Spectral estimation by means of overlapped fast Fourier transform processing of windowed data," NUSC Tech. Rep. 4169, Oct. 13, 1971.

[3] —, "Estimation of cross-spectra via overlapped fast Fourier transform processing," NUSC Tech. Rep. 4169-S, July 11, 1975.

[4] L. R. Rabiner and J. B. Allen, "Short-time Fourier analysis techniques for FIR system identification and power spectrum estimation," *IEEE Trans. Acoust., Speech, Signal Processing,* vol. ASSP-27, pp. 182-192, Apr. 1979.

[5] —, "On the implementation of a short-time spectral analysis method for system identification," *IEEE Trans. Acoust., Speech, Signal Processing*, vol. ASSP-28, pp. 69-78, Feb. 1980.

[6] J. B. Allen and L. R. Rabiner, "Unbiased spectral estimation and system identification using short-term spectral analysis methods," *Bell Syst. Tech. J.*, vol. 58, no. 8, pp. 1743-1763, Oct. 1979.

[7] D. H. Youn and V. J. Mathews, "On using the short-time unbiased spectrum estimation algorithm for estimating time delays and magnitude-squared coherence functions," in *Proc. ASSP Workshop on Spectrum Estimation-II,* Tampa, FL, Nov. 10-11, 1983, pp. 60-64.

[8] A. H. Nuttall and G. C. Carter, "Special estimation using combined time and lag weighting," *Proc. IEEE,* vol. 70, pp. 1115-1125, Sept. 1982.

[9] H. Rohling and J. Schuermann, "Discrete time window functions with arbitrarily low sidelobe level," *Signal Processing,* vol. 5, pp. 127-138, 1983.

[10] J. S. Bendat and A. G. Piersol, *Measurement and Analysis of Random Data.* New York: Wiley, 1966, p. 265.

[11] F. J. Harris, "On the use of merged, overlapped and windowed FFT's to generate synthetic time series data with a specified power spectrum," in *Proc. Sixteenth Asilomar Conference on Circuits, Systems and Computers,* Pacific Grove, CA, Nov. 8-10, 1982, pp. 316-321.

[12] J. B. Allen, "Short-time spectral analysis, synthesis, and modification by discrete Fourier transform," *IEEE Trans. Acoust., Speech, Signal Processing,* vol. ASSP-25, pp. 235-238, June 1977.

[13] F. J. Harris, "On the use of windows for harmonic analysis with the discrete Fourier transform," *Proc. IEEE,* vol. 66, pp. 51-83, 1978.

[14] A. H. Nuttall, "Some windows with very good sidelobe behavior," *IEEE Trans. Acoust., Speech, Signal Processing,* vol. ASSP-29, pp. 84-91, Feb. 1981.

[15] D. F. Elliot and K. R. Rao, *Fast Transforms: Algorithms, Analysis, Applications.* New York: Academic, 1981.

[16] D. Middleton, *An Introduction to Statistical Communication Theory.* New York: McGraw-Hill, 1960, p. 343.

[17] A. H. Nuttall, "Spectral analysis via quadratic frequency-smoothing of Fourier transformed, overlapped, weighted data segments," NUSC Tech. Rep. 6459, June 1, 1981.

V. John Mathews (S'82-M'85) was born in Nedungadappally, Kerala, India, in 1958. He received the B.E. (Hons.) degree in electronics and communication engineering from the University of Madras, India, and the M.S. and Ph.D. degrees in electrical and computer engineering from the University of Iowa, Iowa City, in 1980, 1981, and 1984, respectively.

From 1980 to 1984 he held a Teaching-Research Fellowship at the University of Iowa, where he is currently a Visiting Assistant Professor with the Department of Electrical and Computer Engineering. His research interests include spectrum estimation, adaptive filtering, and image processing.

Dae-Hee Youn (S'78-M'82) was born in Chungju, Korea, in 1951. He received the B.E. degree in electronic engineering from Yonsei University, Seoul, Korea, in 1977, and the M.S. and Ph.D. degrees from Kansas State University, Manhattan, in 1979 and 1982, respectively.

From 1979 to 1982, he worked as a Research Associate with the Department of Electrical Engineering, Kansas State University. He is currently with the Department of Electrical and Computer Engineering, University of Iowa, Iowa City. His present interests are in the applications of adaptive filtering, time delay estimation, spectrum estimation, and speech/seismic signal processing.

Dr. Youn is a member of Tau Beta Pi and Phi Kappa Phi.